

# Stability of Variability Features Computed from Fetal Heart Rate with Artificially Infused Missing Data

J Spilka<sup>1</sup>, V Chudáček<sup>1</sup>, M Burša<sup>1</sup>, L Zach<sup>1</sup>, M Huptych<sup>1</sup>, L Lhotská<sup>1</sup>, P Janků<sup>2</sup>, L Hruban<sup>2</sup>

<sup>1</sup>Faculty of Electrical Engineering, Czech Technical University in Prague, Czech Republic

<sup>2</sup>Obstetrics and Gynaecology Clinic, University Hospital in Brno, Czech Republic

## Abstract

*Fetal heart rate (FHR) is usually the only measurement acquired directly from the fetus during delivery; therefore, any distortion leading to a corrupted signal means difficulties for fetal surveillance.*

*Obstetricians use morphological features for evaluation of FHR that are usually estimated visually. Other type of features are those that are either difficult to estimate visually or can not be estimated by naked eye at all.*

*In this paper we examined several STV (short), LTV (long term variability) features and one nonlinear feature. We compared features for an undistorted and distorted signal with missing samples. We analyzed feature's stability with respect to acquisition technique (ultrasound measurement, direct ECG measurement).*

*The stability of STV indices were almost identical except standard STV, De Haan index, and Yeh index. These indices changed markedly with increasing percentage of missing samples; Yeh index decreased up to 70% of its nominal value and De Haan index increased up to 350%; this behavior held for FHR recorded using ultrasound measurement and even for FHR directly computed from fetal ECG. This relationship was present for beat-to-beat variability and disappeared for epoch-to-epoch variability.*

## 1. Introduction

Fetal heart rate (FHR) is used together with uterine contractions in the form of cardiotocography measurement for fetal surveillance. FHR is the sole information channel available during the delivery for obstetricians; therefore, any distortion to the FHR signal that subsequently distorts features used for the FHR description could be crucial for obstetricians decision making as well as for automatic evaluation.

In this paper, we focused on FHR distortion, caused by variety of reasons (e.g. fetal or maternal movements, misplaced electrode etc.), leading to corrupted or missing signal. Even though the missing intrapartum FHR is com-

mon (0-40% missing for ultrasound measurement and 0-10% for the direct measurement [1]), there are no guidelines stating when a signal is unusable either for visual inspection or for automatic analysis. Usual empirical value given by clinicians is 50% though there is no evidence of effect of such a distortion on the commonly used indices for FHR evaluation such as short and long term variability (STV/LTV). Especially the STV is important since it is widely used in the clinical practice. The STV represents oscillation around FHR baseline in short period of time, large variability correspond to well functioning autonomic nervous system and shows that fetus is able to adapt to changing environment. On the other hand, decreased variability suggest developing metabolic acidemia [2].

The STV also changes with acquisition technique used (ultrasound Doppler (US), direct fetal ECG measurement (DECG)) [3]. When using US the FHR has lower quality and, more importantly, the measurement based on correlation smooths successive values of FHR leading to decreased beat-to-beat variability.

In this paper we evaluated several STV/LTV indices and one nonlinear feature used for FHR assessment. We computed features for the undistorted signal and then added artificial distortion (missing samples) in different patterns (up to 5000 combination, when possible) and percentage (0-50%). We also compared values of features for undistorted and distorted FHR with respect to the acquisition technique.

## 2. Methods

### 2.1. Experimental data

We used cardiotocograms (CTG) signals acquired at Obstetrics and Gynaecology Clinic, University Hospital in Brno, Czech Republic using device STAN S21 during 2010 – 2012; all women signed informed consent. The set consisted of 443 selected records with selection criteria as follows: one fold pregnancy, vaginal delivery, pH > 7.15. The main clinical characteristics of the selected set were: gestational age of  $39.98 \pm 1.17$  (minimum 38, maximum

42); Apgar score in the fifth minute  $9.29 \pm 0.83$  (minimum 7, maximum 10); pH (mean  $\pm$  standard deviation)  $7.27 \pm 0.07$ .

The acquired CTG (both US and DECG) were uniformly sampled with the sampling frequency  $f_s = 4$  Hz.

## 2.2. Data preprocessing

The chosen signals were within 90 minutes before delivery with second stage length of 30 minutes at maximum. In this work we selected 3434 segments with selection criteria as follows: FHR within 1<sup>st</sup> stage of labor, 5 minutes long, less than 5% of missing signal and no decelerations or part of decelerations. The decelerations were defined using FIGO guidelines [4]. The 2351 segments were extracted from US measurement and 1083 from DECG measurement.

## 2.3. Signal processing

Artefacts in the FHR were rejected using algorithm developed by Bernardes et al. [5]. The original FHR signals were artificially distorted by inducing missing samples with different patterns. The patterns of missing data were generated using random permutation (maximum 5000 combination, when possible). The percentage of missing samples was in range 0-50%.

The methods for FHR features extraction (STV/LTV) should be able to compute across the missing samples; however such design and implementation is cumbersome. Ideally the missing samples should be interpolated with new samples that correspond to real FHR (e.g. generated by a dynamical model of FHR). In the worst case scenario the missing samples should be linearly interpolated. In order to avoid any other source of possible distortion we used the later approach.

## 2.4. Features

Obstetricians use morphological features (accelerations, decelerations, baseline value etc.) for evaluation of CTG signals. These features are defined by guidelines [4] and usually estimated visually. Another type of features are those that are either difficult to visually estimate or can not be estimated by naked eye at all. This category includes short/long term variability and also variety of other features (frequency, entropy, complexity, and fractal dimension). We decided to compare several STV and LTV features. We also include fractal dimension computed by Higuchi method since it could be used for estimation of short and long time variability [6].

Let  $x(i)$  be defined as the FHR signal for  $i = 1, 2, \dots, N$  where  $N$  is a length of FHR. The  $x(i)$  is expressed in beats per minute (bpm). Another, correspond-

ing expression of  $x(i)$  used in this work are known as RR series with time increments  $T(i)$  (in seconds). As noted in [7] the short variability computed using  $x(i)$  and  $T(i)$  is not always the same because of dependence on a value of FHR mean utilized in some variability computation.

### 2.4.1. Short term variability (STV)

There are two principal ways how to estimate short term variability depending on signal acquisition technique. For the DECG the beat-to-beat variability approach is used, on the other hand, when CTG is acquired using Doppler ultrasound technique, there is no real beat-to-beat (BB) variability because of intrinsic smoothing due to correlation based technique. Instead epoch-to-epoch (EE) variation is used when the FHR is averaged over short period of time. Mantel et al. [8] suggests 2.5 sec for averaging while in the Sonicaid 8000 system the period of 3.75 sec is used [9]. To highlight the difference between BB and EE, we first computed STV for BB and then also for EE. Note that for Sonicaid 8000 we did not omit implicit averaging embedded in the formula. Equations for computation of STV are presented for BB variability (indices are marked with superscript <sup>BB</sup>, e.g.  $STV^{BB}$ ) but also holds for EE variability (marked with <sup>EE</sup>, e.g.  $STV^{EE}$ ) computed from averaged signal (time period 2.5 sec.); only samples  $i$  were replaced by averaged subintervals. The STV is estimated for signal of length 60 sec.; for longer signals the 60 sec. estimations are averaged.

**STV:** (standard beat-to-beat variability)

$$STV^{BB} = \frac{1}{N} \sum_{i=1}^{N-1} |T(i+1) - T(i)| \quad [\text{ms}]$$

**STV – De Haan** [10]: (STV-HAA<sup>BB</sup>)

$$STV\text{-HAA}^{BB} = \text{IQR}(\arctg\left(\frac{T(i)}{T(i-1)}\right)) \quad [\text{a.u.}]$$

**STV-YEH** [11]: (STV-YEH<sup>BB</sup>)

$$STV\text{-YEH}^{BB} = \sqrt{\sum_{i=1}^{N-1} \frac{(D(i) - \bar{T})^2}{N-2}} \quad [\text{ms}],$$

$$\text{where } D(i) = 1000 \cdot \frac{T(i) - T(i+1)}{T(i) + T(i+1)}, \bar{T} = \frac{1}{N-1} \sum_{i=1}^{N-1} T(i)$$

**Standard deviation:** (STV-SD<sup>BB</sup>)

$$STV\text{-SD}^{BB} = \sqrt{\frac{1}{N-1} \sum_{i=1}^N (T(i) - \bar{T})^2} \quad [\text{ms}],$$

$$\text{where } \bar{T} = \frac{1}{N} \sum_{i=1}^N T(i)$$

**Sonicaid 8000** [9]: (Sonicaid)

$$\text{Sonicaid} = \frac{1}{h} \sum_{s=1}^h |R(s+1) - R(s)| \quad [\text{ms}],$$

where  $R(s) = \sum_{i=1}^r (T(i+1) - T(i)) / \bar{s}$ ,  $h$  is number of subintervals in 60 sec ( $h = 60/r$ ),  $r$  is number of intervals RR in 3.75 sec  $r = f_s \cdot 3.75$ , and  $\bar{s} = \bar{T}$  in 3.75 sec.

## 2.4.2. Long term variability (LTV)

Long term variability is computed over 60 seconds and there is no need of averaging the signal in 60 seconds as for the STV. For longer FHR than 60 sec. estimations of LTV are averaged over each 60 sec.

LTV: (also referred as the Delta value)

$$LTV = T_{max} - T_{min} \quad [\text{ms}],$$

where:  $T_{max/min} = \max/\min\{T(1), \dots, T(N)\}$

LTV – De Hann [10]: (LTV-HAA)

$$LTV\text{-HAA} = \text{IQR}(\sqrt{T(i-1)^2 + T(i)^2}) \quad [\text{a.u.}]$$

Standard deviation: (LTV-SD)

The same equation as for the STV-SD.

## 2.4.3. Higuchi's fractal dimensionn (FD)

The Higuchi method [6] calculates fractal dimension from the estimated length of a signal. From an original signal  $x(i)$  a new signal,  $X_k^m$ , is constructed:  $X(m), X(m+k), X(m+2k), \dots, X(m + [(N-m)/k])$  ( $m = 1, 2, \dots, k$ ), where  $[\ ]$  denotes the Gauss' notation,  $m$  defines the initial time, and  $k$  the time interval. The  $k$  represents time displacement and the number of new created subsets is equal to  $k$ . Then for each  $m$  the length  $L_m(k)$  of  $X_k^m$  is computed. The length of the curve for time interval  $k$ ,  $\langle L(k) \rangle$ , is defined as the average value over  $k$  set of  $L_m(k)$ :  $\langle L(k) \rangle = \sum_{m=1}^k L_m(k)/k$ . The computed curve length  $\langle L(k) \rangle$  for different  $k$  is related to the fractal dimension  $D$  by the exponential formula  $\langle L(k) \rangle \propto k^{-D}$ . The fractal dimension is estimated as a slope of fitted regression to log-log plot of  $\langle L(k) \rangle$  versus  $k$ . Two scaling regions were estimated on log-log plot, corresponding to STV and LTV, respectively [6]. The separation (critical) time was 3s.

## 3. Results

First we tested how the individual features behave with increasing percentage of missing samples. The relationships to missing data for standard STV, STV-HAA, and for Higuchi fractal dimension are shown in Figures 1, 2 and 3, respectively.

The detailed results for all features are present in Tables 1 and 2. In the former table the features were extracted from FHR measured using US and in the later table the DECG measurement was used. In the tables the  $\gamma_0$  express feature value for original FHR (i.e. without missing samples), the  $\Delta(\gamma_{50} - \gamma_0)$  represents difference between original FHR and FHR with 50% of missing samples. The last column in tables  $100 \cdot (\gamma_{50}/\gamma_0)$  shows relative change in feature value (in percentage).

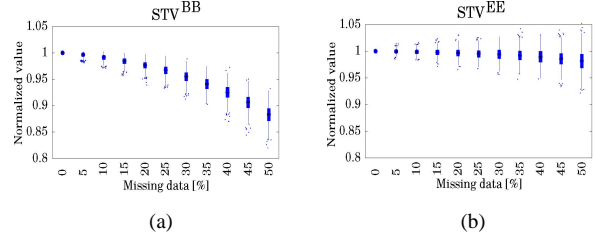


Figure 1. Standard  $STV^{BB}$ ,  $STV^{EE}$  for increasing percentage of missing samples (US measurement).

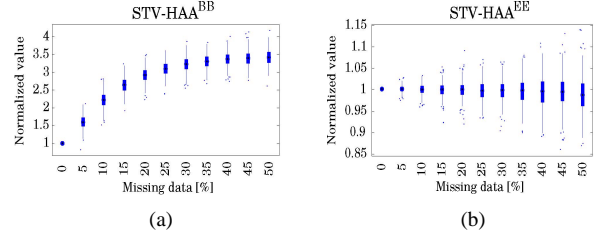


Figure 2.  $STV\text{-HAA}^{BB}$  and  $STV\text{-HAA}^{EE}$  for increasing percentage of missing samples (US measurement).

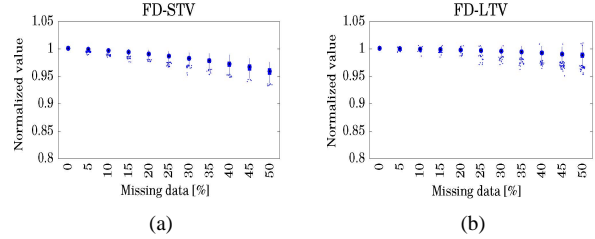


Figure 3. FD-STV and FD-LTV for increasing percentage of missing samples (US measurement).

Table 1. Comparison of features values for US measurement. The  $\gamma_0$  is expressed in median with (25th percentil; 75th percentil). The others are presented as the mean  $\pm$  standard deviation.

	$\gamma_0$	$\Delta(\gamma_{50} - \gamma_0)$	$100 \cdot (\gamma_{50}/\gamma_0)$
$STV^{BB}$	1.6 (1.1;2.2)	$-0.3 \pm 0.1$	$-15.6 \pm 7.7$
$STV^{EE}$	6.8 (4.4;10.5)	$-0.1 \pm 0.2$	$-1.5 \pm 1.2$
$STV\text{-HAA}^{BB}$	0.03 (0.00;0.05)	$0.08 \pm 0.05$	$218.8 \pm 146.6$
$STV\text{-HAA}^{EE}$	0.7 (0.4;1.0)	$0.0 \pm 0.0$	$-1.2 \pm 2.6$
$STV\text{-YEH}^{BB}$	3.7 (2.5;5.3)	$-1.2 \pm 0.7$	$-29.1 \pm 4.3$
$STV\text{-YEH}^{EE}$	11.1 (7.1;16.7)	$-0.1 \pm 0.2$	$-1.6 \pm 1.1$
$STV\text{-SD}^{BB}$	16.0 (10.5;23.7)	$-0.3 \pm 0.3$	$-1.4 \pm 0.7$
$STV\text{-SD}^{EE}$	14.6 (9.7;22.4)	$-0.1 \pm 0.1$	$-0.4 \pm 0.4$
Sonicaid	7.9 (5.0;12.2)	$-0.1 \pm 0.1$	$-0.9 \pm 0.8$
LTV	65.7 (44.6;100.9)	$-1.6 \pm 1.5$	$-2.2 \pm 1.4$
LTV-HAA	25.7 (17.6;38.9)	$-0.2 \pm 0.5$	$-0.7 \pm 1.4$
LTV-SD	15.1 (10.1;23.4)	$-0.3 \pm 0.2$	$-1.4 \pm 0.7$
FD-STV	1.3 (1.2;1.4)	$-0.1 \pm 0.0$	$-4.8 \pm 2.2$
FD-LTV	1.7 (1.5;1.7)	$-0.1 \pm 0.0$	$-0.9 \pm 0.3$

Table 2. Comparison of features values for (DECG) measurement technique. For the details on the abbreviations used see the previous table.

	$\gamma_0$	$\Delta(\gamma_{50} - \gamma_0)$	$100 \cdot (\gamma_{50}/\gamma_0)$
STV <sup>BB</sup>	2.2 (1.5;3.5)	-0.5 ± 0.2	-19.1 ± 6.7
STV-HAA <sup>BB</sup>	0.03 (0.00;0.06)	0.12 ± 0.08	246.5 ± 142.6
STV-YEH <sup>BB</sup>	4.9 (3.5;7.5)	-1.8 ± 1.0	-30.7 ± 3.1
STV-SD <sup>BB</sup>	17.2 (11.1;28.1)	-0.4 ± 0.4	-1.7 ± 0.9
Sonicaid	8.7 (5.5;15.0)	-0.1 ± 0.2	-0.7 ± 1.0
LTV	76.7 (50.7;127.7)	-2.4 ± 1.7	-2.8 ± 1.6
LTV-HAA	30.3 (19.7;47.8)	-0.3 ± 0.7	-0.6 ± 1.5
LTV-SD	17.2 (11.1;28.1)	-0.4 ± 0.4	-1.7 ± 0.8
FD-STV	1.4 (1.3;1.5)	-0.1 ± 0.0	-6.0 ± 1.9
FD-LTV	1.7 (1.6;1.8)	0.0 ± 0.0	-0.9 ± 0.3

The tables show that for 50% of missing data the values of features decrease expect for index STV-HAA, which increases up to  $\approx 350\%$  of its nominal value (computed from original FHR). The indices STV<sup>BB</sup>, STV-YEH<sup>BB</sup> decrease markedly up  $\approx 85\%$  and  $\approx 70\%$ , respectively. The other features decreased including LTV and Higuchi fractal dimension decreased at most 6%. This holds irrespective of measurement method used (US, DECG).

#### 4. Discussion and conclusion

In this paper we examined the stability of several variability features used for evaluation of FHR. We focused on the influence of missing samples to features' value.

The stability of features was almost identical with three exceptions. Standard STV (STV<sup>BB</sup>) and Yeh index (Yeh<sup>BB</sup>) decreased markedly to  $\approx 85\%$  and  $\approx 70\%$  for the US measurement and to  $\approx 80\%$  and  $\approx 70\%$  for the DECG measurement. On the other hand, the STV-HAA<sup>BB</sup> increased up to  $\approx 350\%$  of its nominal value. The rest of examined features decreased about 6% at most.

It is clear that epoch-to-epoch variability should be favored for the US measurement for the following reasons: first, there is no real beat-to-beat variability for US measurement and, second, the epoch-to-epoch variability is more robust to the missing data. For the DECG measurement the indices STV<sup>BB</sup>, Yeh<sup>BB</sup>, and STV-HAA<sup>BB</sup> should be able to estimate true BB variability but fail to do so when signal is corrupted.

Even though that indices STV<sup>BB</sup>, Yeh<sup>BB</sup>, and STV-HAA<sup>BB</sup> change its nominal value for missing samples this type of behavior could be also beneficial when slight changes in FHR occurs. These changes could reflect change in fetal behavior/state and could be used for clinical evaluation.

#### Acknowledgements

This work has been supported by the ČVUT Grant SGS10/279/OHK3/3T/13 and by the research programs No. NT11124-6/2010 Cardiocography evaluation by means of artificial intelligence of the Ministry of Health Care.

#### References

- [1] Bakker PC, Colenbrander GJ, Verstraeten AA, Van Geijn HP. The quality of intrapartum fetal heart rate monitoring. *Eur J Obstet Gynecol Reprod Biol Sep 2004;116(1):22–27.*
- [2] Street P, Dawes GS, Moulden M, Redman CW. Short-term variation in abnormal antenatal fetal heart rate records. *Am J Obstet Gynecol Sep 1991;165(3):515–523.*
- [3] Jezewski J, Wrobel J, Horoba K. Comparison of Doppler ultrasound and direct electrocardiography acquisition techniques for quantification of fetal heart rate variability. *IEEE Trans Biomed Eng 2006;53(5):855–864. ISSN 0018-9294.*
- [4] FIGO. Guidelines for the use of fetal monitoring. *International Journal of Gynecology Obstetrics 1986;25:159–167.*
- [5] Bernardes J, Moura C, de Sa JP, Leite LP. The Porto system for automated cardiocographic signal analysis. *J Perinat Med 1991;19(1-2):61–65.*
- [6] Higuchi T. Approach to an irregular time series on the basis of the fractal theory. *Phys D 1988;31(2):277–283. ISSN 0167-2789.*
- [7] Cesarelli M, Romano M, Bifulco P. Comparison of short term variability indexes in cardiocographic foetal monitoring. *Comput Biol Med Feb 2009;39(2):106–118.*
- [8] Mantel R, van Geijn HP, Caron FJ, Swartjes JM, van Woerden EE, Jongsma HW. Computer analysis of antepartum fetal heart rate: 1. baseline determination. *Int J Biomed Comput May 1990;25(4):261–272.*
- [9] Pardey J, Moulden M, Redman CWG. A computer system for the numerical analysis of nonstress tests. *Am J Obstet Gynecol May 2002;186(5):1095–1103.*
- [10] de Haan J, van Bommel J, Versteeg B, Veth A, Stolte L, Janssens J, Eskes T. Quantitative evaluation of fetal heart rate patterns. i. processing methods. *European Journal of Obstetrics and Gynecology and Reproductive Biology 1971;1(3):95–102. Cited By (since 1996) 13.*
- [11] Yeh SY, Forsythe A, Hon EH. Quantification of fetal heart beat-to-beat interval differences. *Obstet Gynecol Mar 1973; 41(3):355–363.*

Address for correspondence:

Jiří Spilka  
Department of Cybernetics, Czech Technical University in Prague, Technická 6, 166 37 Praha 6, Czech Republic  
spilka.jiri@fel.cvut.cz